Research Article | Vol. 13, No. 3 / 1 Mar 2022 / Biomedical Optics Express 1485

Biomedical Optics EXPRESS

Corneal transparency and scleral opacity arises from the nanoarchitecture of the constituent collagen fibrils

SNOW H. TSENG,[1,5] CHIH-YAO YANG,[1] JIA-HAO LI,[1] YUNG-MING JENG,[2] JANAKA C. RANASINGHESAGARA,[3,4] AND VASAN VENUGOPALAN[3,4,*]

[1] Graduate Institute of Photonics and Optoelectronics, National Taiwan University, Taipei, 10617, Taiwan
[2] Department of Pathology, National Taiwan University Hospital, National Taiwan University, Taipei, 10617, Taiwan
[3] Department of Chemical and Biomolecular Engineering, Univ. of California, Irvine, CA. 92697, USA
[4] Beckman Laser Institute and Medical Clinic, Univ. of California, Irvine, CA. 92697, USA
[5] stseng@ntu.edu.tw
[*] vvenugop@uci.edu

Abstract: While human scleral and corneal tissues possess similar structural morphology of long parallel cylindrical collagen fibrils, their optical characteristics are markedly different. Using pseudospectral time-domain (PSTD) simulations of Maxwell's equations, we model light propagation through realistic representations of scleral and corneal nanoarchitecture and analyze the transmittance and spatial correlation in the near field. Our simulation results provide differing predictions for scleral opacity and corneal transparency across the vacuum ultraviolet to the mid-infrared spectral region in agreement with experimental data. The simulations reveal that the differences in optical transparency between these tissues arise through differences in light scattering emanating from the specific nanoscale arrangement and polydispersity of the constituent collagen fibrils.

© 2022 Optica Publishing Group under the terms of the Optica Open Access Publishing Agreement

1. Background

The human eye consists of two collagen-based tissues: sclera and cornea. Cornea and sclera ultrastructure possess very similar geometrical features as both consist of multiple layers of collagen fibrils that form parallel lamellar bundles [1]. Despite this similarity, the sclera and cornea exhibit drastically different optical properties in the visible spectral region: sclera is largely opaque, while the cornea is transparent. Together, the sclera and cornea form the outer fibrous tunic of the eye and provide the mechanical support to withstand internal and external forces and maintain the shape of the eyeball [1]. With its external surface appearing white, the opaque sclera covers nearly the entire surface of the eyeball. The cornea is located centrally at the anterior of the external tunic and its transparency supports visible light transmission into the interior of the eye.

The mechanistic origin underlying the stark difference in appearance between these two tissues, despite their similar composition and morphology, has been of longstanding interest to the scientific community. Research into corneal transparency dates back to early 19th century when it was generally believed that cornea transparency was due to a uniform refractive index [2]. In 1953, Aurell and Holmgren reported the first refractive index measurements for corneal fibrils and interstitial fluid, obtaining values of 1.547 and 1.342, respectively [3]. This revelation of differing refractive indices of the corneal tissue constituents completely overturned the general understanding of corneal transparency. In 1957, Maurice proposed the lattice theory of corneal transparency [4] by asserting that incident light scattered by the corneal collagen fibrils

#444832 https://doi.org/10.1364/BOE.444832
Journal © 2022 Received 5 Oct 2021; revised 3 Feb 2022; accepted 6 Feb 2022; published 15 Feb 2022

Biomedical Optics EXPRESS

constructively interfere in the original direction of propagation, but de-constructively interfere in other directions. Furthermore, based on the positioning of collagen fibrils, he noted that the transparency is the result of collagen fibrils of uniform size positioned into a hexagonal lattice. In 1969, Hart and Farrell [5] suggested that short-range order of the corneal collagen fibrils causes destructive interference of light in directions that deviate from the propagation of an incident wavefront. Moreover, electron microscope images confirmed that "short-range order" indeed exists in the cornea, which may be essential to transparency [2]. Transmission electron microscopy images depicting the geometrical structure of the sclera and cornea are shown in Fig. 1. Goldman and Benedek [6,7] suggested that the difference in spacing between scleral collagen fibrils and corneal collagen fibrils may account for the scleral opacity and corneal transparency.

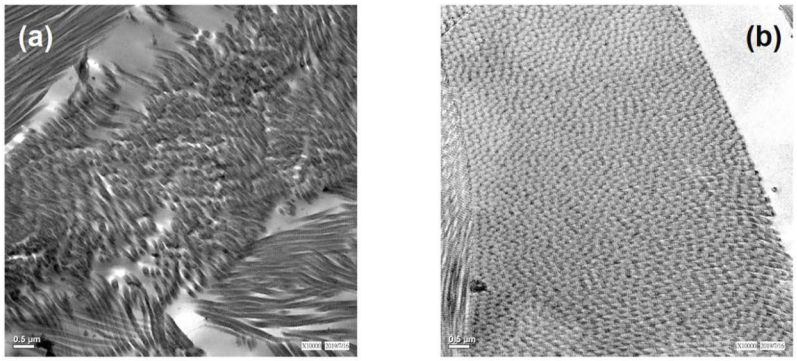

Fig. 1. Cross-sectional images of the sclera and cornea acquired with a JEOL JEM-1400 transmission electron microscope. Both (a) scleral and (b) corneal tissues consist of long, parallel collagen fibrils clustered into a layer structure. The scleral collagen fibrils are polydisperse and disordered, whereas the corneal collagen fibrils have a uniform diameter and run parallel within the lamellae. Scale bar = 500nm. **[Courtesy of the Department of Pathology, National Taiwan University Hospital.]**

To date, these hypotheses have not been examined using rigorous simulation of electromagnetic propagation within realistic computational models of corneal and scleral tissues. In this study we designed and executed rigorous simulations of light propagation using Maxwell's equations in computational representations of ocular tissue, to investigate whether the differences in scleral and corneal nanoarchitecture result in different light scattering characteristics that lead to scleral opacity and corneal transparency.

2. Methods

Sclera and cornea both consist of layers of parallel collagen fibrils. In each lamellar layer, the scleral/corneal collagen fibrils run parallel in a uniform direction. Scleral collagen fibrils are polydisperse with diameters ranging from 25 nm to 300 nm [8–10]. By contrast, the corneal collagen fibrils are nearly uniform in size (30.8 ± 1nm in diameter for young people and 32.2 ± 1nm in diameter for older people) [1,11]. To analyze the influence of the nanoscale scleral/corneal architecture on light transmission, we performed 2D near-field simulations to analyze continuous-wave (CW) light propagation through computational representations of scleral and corneal tissues.

We model both sclera and cornea as a cluster of infinitely long dielectric cylinders with refractive index $n = 1.504$ embedded within a background medium of refractive index $n = 1.345$. The nanoarchitecture of the sclera is modeled as a polydisperse suspension of collagen fibrils of uniform distribution with diameter ranging between 29.74 nm and 297.4 nm positioned randomly

Biomedical Optics EXPRESS

in space [11]. The nanoarchitecture of the cornea is modeled as a monodisperse suspension of collagen fibrils of uniform distribution with diameter of 29.74 nm with an edge-to-edge spacing no less than 59.48 nm. For sclera, we chose mixed diameters consisting of 29.74 nm, 59.48 nm, 89.22 nm, 118.96 nm, 148.7 nm, 178.44 nm, 208.18 nm, 237.92 nm, 267.66 nm, and 297.4 nm. The number of fibrils of each diameter are averaged based on cross-sectional area. The total number of collagen fibrils were chosen to ensure the average refractive index of the entire scattering medium remains constant. By fixing the volume fraction, the overall average refractive index of the scleral and corneal models is identical. Schematics depicting the cross-sectional view of the computational representation of the scleral and corneal tissue layers are shown in Fig. 2.

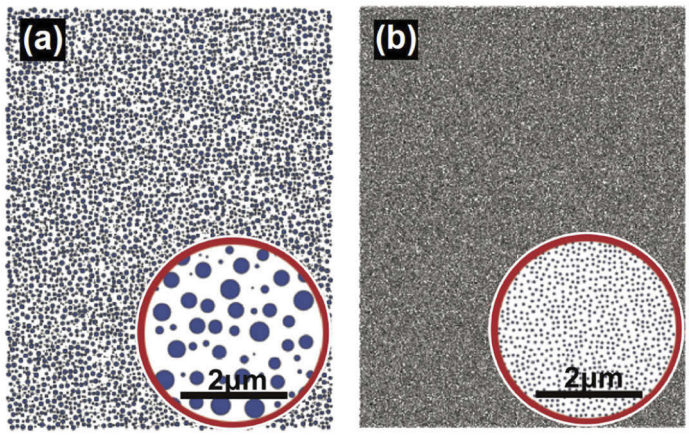

Fig. 2. Modeling light propagation through computational representations of: (a) sclera and (b) cornea. In a 22 μm × 30 μm region, the scattering medium consists of: (a) sclera: 6000 mixed-size collagen fibrils with diameter ranging from 29.74 nm to 297.4 nm randomly positioned in space, (b) cornea: 86775 uniform collagen fibrils with a diameter of 29.74 nm randomly positioned in space. The refractive index of the collagen fibrils is $n_c = 1.504$ immersed in extrafibrillar substance with a refractive index of: $n_b = 1.345$.

To accurately model light propagation through a macroscopic scattering medium, we employ a two-dimensional (2-D) pseudospectral time-domain (PSTD) simulation [12]. Based upon numerical solutions of Maxwell's equations, the PSTD algorithm is robust and advantageous for modeling large-scale light scattering phenomenon [13]. Similar to the finite-difference time-domain (FDTD) simulation technique, the temporal derivatives are calculated via leap-frog finite difference scheme. The spatial derivatives are acquired via discrete Fourier transforms and a factor of jk_x is multiplied in the frequency domain that provides spatial derivatives of the field throughout the computational domain. Along a given direction, the spatial derivative of the electric field is given by [11]:

$$\left\{ \left. \frac{\partial \boldsymbol{E}}{\partial x} \right|_i \right\} = -\mathcal{F}^{-1}\{jk_x \cdot \mathcal{F}[\boldsymbol{E}_i]\}, \tag{1}$$

where $\boldsymbol{E}$ is the electric field vector, k_x is the wave number, and $\mathcal{F}$ represents the Fourier transform. While maintaining accuracy comparable to the conventional FDTD, the PSTD technique reduces the required computer memory storage and the running-time by a factor of 8^D for simulation of large electromagnetic wave interaction models in D dimensions that does not have geometric details or material inhomogeneities smaller than one-half wavelength [12]. The temporal derivatives are calculated using a central difference scheme similar to the FDTD technique.

Biomedical Optics EXPRESS

Instead of using central difference scheme of nearby points to approximate the derivative, the PSTD technique achieves accuracies comparable to the FDTD technique using a grid of only two spatial samples per wavelength as compared to 20 spatial samples per wavelength for the FDTD technique. The coarse spatial grid points enables accurate modeling of a light scattering problems on macroscopic length scales. In addition, an anisotropic perfectly matched layer (APML) absorbing boundary condition [14] is utilized to absorb all outgoing waves to simulate an isolated optical system.

Our objective is to investigate the light scattering characteristics of computational representations of corneal tissues (mono-disperse collagen fibrils) vs. scleral tissues (poly-disperse collagen fibrils). Due to the computational cost required to numerically solve Maxwell's equations for light propagation within a macroscopic 3D scattering medium, we consider a 2D computational domain with dimensions 30-µm in height and varying thicknesses in the range of 20–65µm to allow execution of simulations within a modest time frame. While the maximal thickness of the human cornea and sclera are roughly 500 µm and 1000 µm, respectively, our small computational domain is sufficiently large to model these irregular scattering media and identify the nanoarchitectural factors that contribute to transparency/opacity.

Instead of modeling a plane wave of infinite lateral extent, we consider a narrow finite-width continuous wave (CW) light source emitting a plane wave through a scattering medium [15]. The finite-width CW plane wave enables quantitative analysis of both the direction and spatial coherence of light propagation, both of which are essential to examine to assess the degree of optical transparency. The interference of narrow width CW light gradually attenuates as it propagates through vacuum (Fig. 3(a)). The wavelengths we simulate span the vacuum ultraviolet through near infrared spectral regime. We analyze the amplitude profile and lateral spreading of the incident wavefront as it propagates through scleral and corneal tissues. By examining the propagation of the light field through these scattering media, we can quantify both deviations in the propagation direction and the decrease of transmitted light intensity.

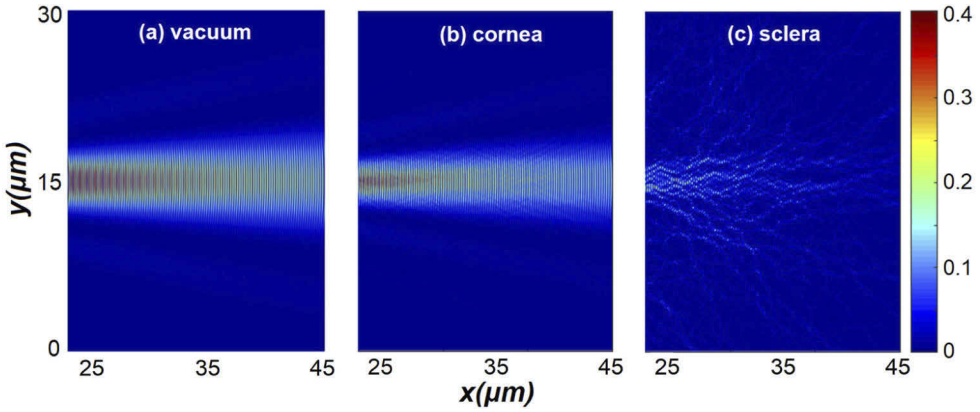

Fig. 3. Intensity distribution of a CW plane wave (λ= 400 nm) in the latter half of 45 µm thick samples of (a) vacuum (b) corneal and (c) scleral media. The initial width of the plane wave is 4 µm and the full dimensions of the computational domain medium is 45 µm thick × 30 µm high. The wavelength of the incident light is 400nm. The scleral sample consists of dielectric cylinders with diameters ranging from 29.74 nm to 297.4 nm. The corneal sample consists of dielectric cylinders of uniform 29.74 nm diameter. The corneal medium supports light propagation in a manner similar to vacuum. By contrast, the scleral geometry hinders light propagation. Differences in light transmittance between corneal and scleral tissue representations become more apparent when considering samples of progressively larger thickness spanning 20–65 µm (Fig. 4).

Biomedical Optics EXPRESS

3. Simulating light propagation through scleral/corneal medium

We model the irradiation and propagation of CW light on representations of scleral (Fig. 2(a)) and corneal (Fig. 2(b)) tissues and compare light propagation through these two tissues with propagation through vacuum. Simulation results show that scleral and corneal tissues exhibit significantly different optical penetration characteristics. Specifically, the plane wave impinging upon corneal tissue is barely deflected and displays propagation similar to that through vacuum (Fig. 3(b)) whereas the scleral tissue severely scatters the incident wave front into all directions (Fig. 3(c)).

3.1. Effect of medium thickness

First, we model light propagation through scattering medium of various thicknesses in the near field. The light propagation is nearly unaltered when passing through the corneal geometry. However, light propagation in scleral geometry is severely randomized into all directions. Note that due to irregular scattering, it is sometimes possible that the summed intensity spikes exceed that in the vacuum as is seen for thicknesses in Fig. 4 for thicknesses in the range of 45–65 µm. It is evident that with increased thickness, the corneal geometry supports light penetration similar to that in vacuum, as opposed to the opacity of the scleral geometry.

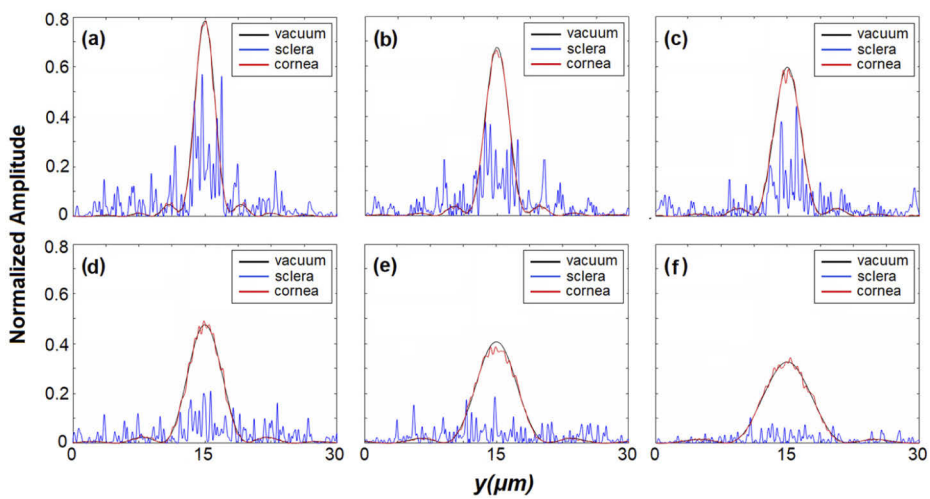

Fig. 4. Comparison of the transmitted light through sclera-like and cornea-like scattering media of thickness: (a) 20 µm, (b) 25 µm, (c) 35 µm, (d) 45 µm, (e) 55 µm, and (f) 65 µm. The wavelength of the incident light is 400 nm. Increased sample thickness results in a progressive reduction of light transmission through the scleral medium, whereas light propagating through corneal medium is minimally affected and comparable to propagation in vacuum.

3.2. Effect of collagen fibril polydispersity

To examine the impact of collagen fibril diameter polydispersity on light transmittance we model light propagation within various populations of absorption-free collagen fibrils with increasing degrees of polydispersity. The modelling of these various fibril clusters is shown in Fig. 5 (upper row, (a)-(e)), ranging from (a) collagen fibrils with a uniform diameter $d = 29.74$ nm, to (e) polydisperse collagen fibrils with diameters d ranging from 29.74 nm to 297.4 nm. In all cases the number of collagen fibrils were adjusted to maintain a constant volume fraction.

Biomedical Optics EXPRESS

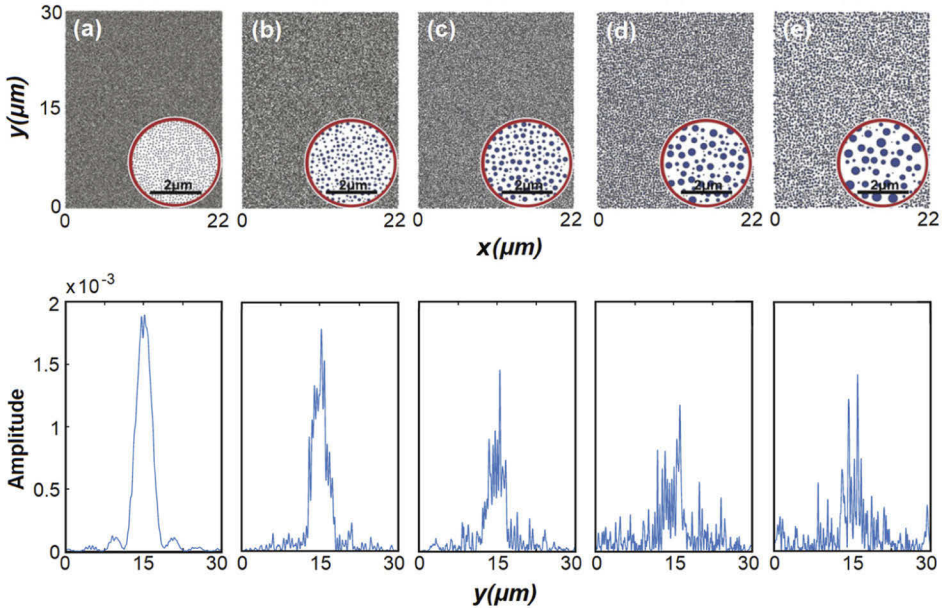

Fig. 5. Modeling light propagation through scattering media of increasing fiber polydispersity. (upper row): (a) A total of $N = 86{,}775$ dielectric cylinders with uniform diameter $d = 29.74$ nm. (b) A total of $N = 30{,}000$ dielectric cylinders with diameter d ranging from 29.74 nm to 89.22 nm. (c) A total of $N = 18{,}000$ dielectric cylinders with diameter d ranging from 29.74 nm to 148.70 nm. (d) A total of $N = 9{,}000$ dielectric cylinders with diameter d ranging from 29.74 nm to 237.92 nm. (e) A total of $N = 6{,}000$ dielectric cylinders with diameter d ranging from 29.74 nm to 297.4 nm. (Lower row): The electric field amplitude of light exiting the 22 μm thick scattering medium. The progression from monodisperse (cornea-like) to polydisperse (sclera-like) media results in reduced light transmission and increased lateral spatial dispersion. The wavelength of the incident light is 400 nm.

As shown in Fig. 5 (lower row), increases in fibril polydispersity result in higher levels of wavefront attenuation and spatial dispersion upon propagation through a 22 μm thick scattering media consisting of a population of collagen fibrils with increased polydispersity.

4. Quantifying the transmittance and spatial coherence

As shown in Fig. 4, the transmitted light intensity propagating through our computational model of scleral tissue decreases rapidly with increased thickness, i.e., thicker scleral samples inhibit light transmission in the forward direction. To quantify the distinctive optical characteristics of scleral and corneal tissues as shown in Fig. 3 and 4, we refer to the astronomical definition of transparency and seeing [16]. For perfect transparency, propagation should occur without wavefront distortion and the detected intensity profile should be highly correlated with the intensity profile of light propagating through vacuum. Transparency requires high transmittance and preservation of spatial coherence of light, i.e., the relative light amplitude that embodies the appearance of an image [14]. To quantify transparency of scattering medium, two wavefront factors must be assessed: (i) transmittance and (ii) spatial coherence. Seeing [17] refers to the amount of degradation along the path to the detector. The strength of seeing is characterized by the angular diameter of the image or seeing disc [18], which refers to the circle over the spread of the signal detected by propagating light through the vacuum.

Biomedical Optics EXPRESS

For light propagating through a scattering medium, the transmittance can be quantified by calculating the ratio of the total light intensity propagating through scattering medium I_m and the total light intensity propagating through vacuum I_v [19]:

$$T = \frac{\int I_m dy}{\int I_v \, dy} \tag{2}$$

The integral is taken over the exiting surface of the slab for light propagating in the "forward" direction: the total light intensity within the y-axis of the seeing disc. We can quantify the transparency of a scattering medium by comparing the FWHM of the total light intensity transmitted through the seeing disc of: (i) light propagated through the scattering medium and (ii) light propagated through vacuum. $T = 0\%$ implies that the medium is completely opaque (blocking all light); $T = 100\%$ implies all light can propagate through the medium without loss. The spatial coherence of light that defines the clarity of the image can be estimated by computing the correlation between the intensity profiles of light propagating through a scattering medium and light propagating through vacuum.

We quantitatively analyze the transmittance T. The amount of light transmitted through the medium by summing up the light intensity in the forward direction, as shown in Fig. 6(a). With increased thickness, transmittance T of light through scleral media is severely attenuated, but, nearly unaffected through corneal media. Notice that like speckle, it is possible the summed intensity spikes up at random locations due to irregular scattering, exceeding the vacuum case. This is seen to occur at slab thicknesses of 35 µm and 45 µm in Fig. 6(a). By calculating the transmittance T, we show that the transmitted light intensity propagating through the computational model of sclera decreases with increased thickness. On the other hand, the transmittance T through the computational model of cornea is nearly unaffected by sample thickness.

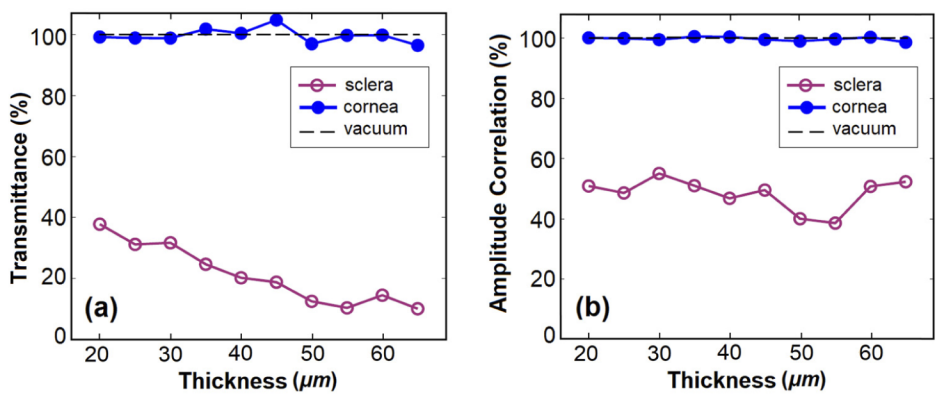

Fig. 6. The transmissivity and spatial coherence of plane wave propagation through sclera vs. cornea. (a) Transmissivity: the total optical intensity transmitted through scleral/corneal medium within the forward FWHM is integrated and compared. (b) Spatial coherence: preservation of the spatial coherence of light is quantified by calculating the correlation of the amplitude profile of light propagating through vacuum. Regardless of thickness, the transmissivity and spatial coherence through cornea is essentially the same as vacuum (perfect transparent case). The wavelength of the incident light is 400 nm.

Of course, the ability to see through an object requires the preservation of spatial coherence; the wavefront of light, points in space having the same phase, contains information of the light source [14]. To assess spatial coherence in the near field, we calculated the correlation between the normalized amplitude profile of light transmitted through scleral geometry/corneal

Biomedical Optics EXPRESS

geometry and vacuum as shown in Fig. 6(b). This result shows that wavefront spatial coherence is preserved upon propagation across 20–65μm thick sections of corneal tissue while it is degraded significantly upon transmission through an equivalent thickness of sclera. It is important to note that spatial coherence of light can be compromised by distortion or aberration without a significant reduction in optical transmission, like a bright yet opaque cloud in the sky. This analysis of the light intensity and spatial coherence in the near field leads to the conclusion that the differences in light scattering produced by differences in collagen fibril polydispersity and their spacing [15], results in the opacity of the sclera and the transparency of cornea. In contrast to scleral tissue, spatial coherence is preserved upon transmission through corneal tissue. This is crucial to transparency and the wavefront characteristics resemble those of light propagating through vacuum.

5. Spectral dependence of transmittance

Next, we analyze the spectral transmittance characteristics of scleral and corneal tissues. It is anticipated that spectral characteristics also originate from the differences in polydispersity between the collagen fibers in sclera as opposed to the monodispersity of the collagen fibrils in cornea [7].

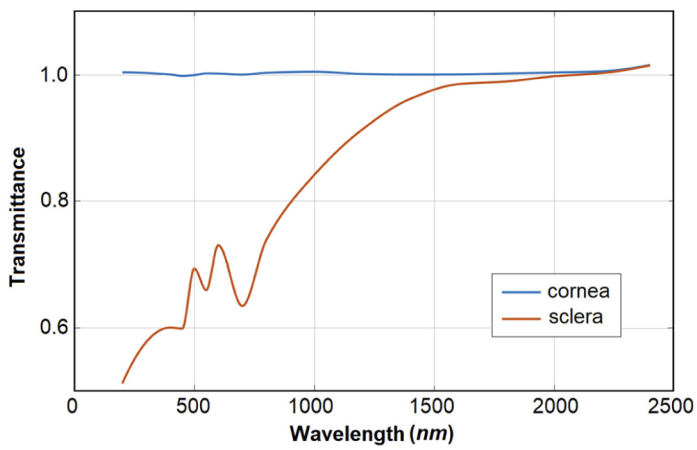

Fig. 7. The transmittance spectra of the computational representations of sclera and cornea tissues as shown in Fig. 2. The incident wavelength ranging from 190 nm up to 2400 nm, covering the optical frequencies. Within a 22 μm×30 μm area, the cornea-like geometry consists of 86775 29.74-nm-diameter dielectric cylinders, whereas the sclera-like geometry consists of 6000 dielectric cylinders with diameter ranging from 29.74 nm to 297.4 nm.

We model wavelengths spanning 190 –2400 nm impinging upon a 22 μm × 30 μm scattering medium consisting of (a) scleral medium: 6000 collagen fibrils with polydisperse diameter ranging from 29.74 nm to 297.4 nm, and (b) corneal medium: 86775 collagen fibrils with a constant diameter 29.74 nm. The transmittance T [19] can be determined by calculating the ratio between the exiting light intensity and the light intensity propagating through vacuum.

$$T = \frac{\sum {E_m}^2}{\sum {E_{m0}}^2} \tag{3}$$

E_m is the amplitude of electromagnetic field after transmitting through the medium, E_{m0} is the amplitude of electromagnetic field before transmitting through the medium. Light is scattered and diffracted as it propagates through the medium, thus E_m and E_{m0} are summed over the forward

Biomedical Optics EXPRESS

direction. As shown in Fig. 7, the differing scattering characteristics produced by scleral vs. corneal fibril nanoarchitecture results in differing wavelength-dependent transmittance properties.

The simulation results show significant attenuation due to the scleral geometry; that is, the scattering caused by the geometry of mixed-diameter collagen fibrils inhibits forward light penetration. In the wavelength range of 190–1000 nm, the scleral geometry inhibits light transmission, whereas the corneal geometry supports nearly perfect transmittance over the entire 190–2400 nm spectral range.

6. Effect of water absorption on the transmittance spectra

We now incorporate the effect of water absorption, which plays a significant role in the optical properties of biological tissue [1,20–22]. To account for water absorption, we treat water as dispersive medium within the scattering simulation. Here, by exploiting the experimentally measured water absorption coefficient for various wavelengths, we simulate CW light scattering and incorporate the water absorption coefficient at various wavelengths. Based upon Beer's law [19], the water absorbance A is expressed as:

$$A = \alpha L c \tag{4}$$

where α is the absorption coefficient, L is the medium thickness, and c is the volume fraction. The absorbance A can be expressed in terms of the transmittance as:

$$A = -\log_{10}\left(\frac{I}{I_0}\right) \tag{5}$$

The relationship between the light intensity I detected following propagation through an absorptive medium and light detected after propagation through absorption-free medium I_0 can be expressed as:

$$I = I_0 * 10^{-\alpha l c} \tag{6}$$

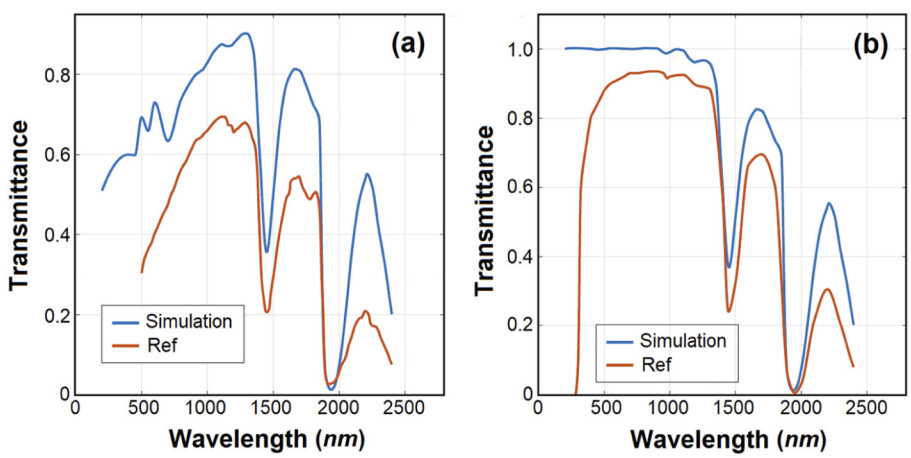

Fig. 8. Simulated transmittance spectra of (a) sclera and (b) cornea as compared to experimentally-measured transmittance spectrum of sclera [23] and cornea [24], respectively. Wavelengths ranging from 190 nm to 2400nm.

Biomedical Optics EXPRESS

After incorporating the water density of corneal or scleral tissues for 30 μm tissue thickness, Eq. (2) becomes:

$$T = 10^{-0.0017\ \alpha} \frac{\int I_m dy}{\int I_v\ dy} \tag{7}$$

where α is given in units of cm^{-1}.

The resulting transmittance spectra incorporate both the scattering and absorption properties of scleral or corneal tissues are shown in Figs. 8(a) and 8(b), respectively, and compared to the experimentally-measured transmittance spectrum of sclera [23], and cornea [24]. The two absorption dips near 1375 nm and 1875 nm are due to water absorption [1]. For wavelengths less than 1200 nm, the transmittance spectrum is dominated by scattering. These simulated transmittance spectra are consistent with spectra obtained from experimental measurements [1,20–24].

7. Discussion

The primary differences between sclera and cornea originate from their different collagen fibril diameters and polydispersity. Corneal and scleral nanoarchitecture consists of layers of bundled monodisperse and polydisperse collagen fibrils, respectively. The fibrils form parallel lamellar bundles for sclera and the posterior cornea, whereas the fibrils within the anterior cornea are interwoven [25]. Even when interwoven, the collagen fibrils are mostly aligned in a bundled parallel configuration. Light impinging upon sclera/cornea is scattered by the collagen fibrils in the near field and propagates into the far field. Since light in the far field essentially contains the near field information, it is, in theory, feasible to analyze far field optical characteristics in the near field. To determine the effect of light scattering caused by microscopic geometry contributes to the overall optical characteristics, we quantify the transmittance and spatial coherence of light in the near field utilizing numerical solutions of Maxwell's equations.

Yet, transmittance alone does not guarantee transparency. For example, a bright cloud in the sky emits ample light but remains non-transparent. By contrast a pair of sunglasses reduce light transmittance, but still allows one to see sharp images. In addition to transmittance, maintenance of spatial coherence is essential for transparency. By analyzing the wavefront of light propagating through scleral/corneal medium vs. light propagating through vacuum, we quantify transparency in the near field. We model light propagation through 2-D computational representations of scleral and corneal tissues, quantify the level of spatial coherence, calculate the transmittance spectra, and compare the results with experimentally measured transmittance spectra. The sclera/cornea transmittance spectra obtained from our computational simulations of Maxwell's Equations are consistent with experimentally measured spectra.

Specific simulation results indicate that the microscopic geometrical structures can collectively affect the macroscopic optical characteristics. For closely packed scattering aggregates, scatterer size, spacing, and polydispersity, each affect the overall light propagation and penetration. These parameters mutually interact, and it is often difficult to unravel the independent influence of each. As qualitatively suggested in [2], the secondary wave phenomenon may provide an explanation for corneal transparency. By analyzing light propagation through computational representations of scleral and corneal tissues, our study provides a framework to enable a firm theoretical foundation for the understanding the impact of optical scattering on tissue transparency/opacity.

We have focused our analysis on the effects of the collagen fibril diameter and degree of polydispersity. Our simulation results demonstrate that individual collagen fibril size and polydispersity both contribute to the transparency, i.e., macroscopic optical characteristics are influenced directly by specific nanoscale arrangement of the tissue constituents. In this manner, our framework can be used as a basis to establish connections between tissue nanoarchitecture and macroscopically observable tissue optical properties.

Biomedical Optics EXPRESS

The reported simulation findings demonstrate the feasibility and utility of near field optical analysis to assess optical transparency. On a broader perspective, specific results show that light scattering caused by microscopic geometrical structure can collectively affect the preservation of phase coherence that results in opacity/transparency.

8. Conclusions

Using a pseudospectral time-domain approach to solving Maxwell's equations combined with accurate nanoscale representations of corneal and scleral tissues, we have modeled light transmission through these tissues and quantified the impacts of collagen fibril diameter, degree of polydispersity, and sample thickness. To investigate how transparency is affected by the specific configurations of collagen fibrils, we analyze in the near field the wavefront amplitude and phase variation of light propagating through sclera/cornea and compare with light propagating through vacuum (perfect transparency).

Even though Maurice's lattice theory [4] may not provide an accurate interpretation of the corneal transparency, our simulation findings show that the spectral characteristics of the scleral transmittance inhibits penetration of all optical wavelengths, which accounts for the white appearance of sclera. Based on the simulation findings, transparency depends on the size of the constituent collagen fibril diameters and is not dependent upon the geometrical arrangement (such as hexagonal lattice distribution). Polydispersity of the fibrils themselves, rather than spacing, appears to determine the optical penetration of specific wavelengths. By incorporating water absorption, the transmittance spectra calculated from the light scattering simulation reported in this paper possess the key features of experimentally measured transmission spectra of both cornea and sclera (Figs. 8(a) and 8(b)). Specifically, the results clearly show that, for the spectral range of 190–2400 nm, the specific corneal nanoarchitecture supports light propagation similar to that in vacuum, whereas scleral nanoarchitecture strongly scatters light into all directions, preventing light transmission. More generally, our analysis demonstrates that the macroscopic optical characteristics of transparency and opacity can be accounted for by scattering caused by the nanoscale architecture and geometrical structure of cornea/sclera.

Funding. National Taiwan University (NTU-ERP-103R89086); Division of Chemical, Bioengineering, Environmental, and Transport Systems (CBET-1805082); National Institute of General Medical Sciences (R21-GM128135); Ministry of Science and Technology, Taiwan (106-2112-M-002-008, 107-2112-M-002-011, 108-2221-E-002-157, 108-2634-F-002-014).

Acknowledgments. We thank Prof. Allen Taflove for his instruction and guidance on running simulations, Prof. Joseph T. Walsh for the inspiration of this research project. We thank Prof. C. Y. Dong, Department of Physics, National Taiwan University, and the support of the Department of Pathology, National Taiwan University Hospital, for providing the tissue sample measurements.

Disclosures. The authors declare that there are no conflicts of interest related to this article.

Data Availability. Data underlying the results presented in this paper are not publicly available at this time but may be obtained from the authors upon reasonable request.

References

1. Y. Komai and T. Ushiki, "The three-dimensional organization of collagen fibrils in the human cornea and sclera," Invest. Ophthalmol. Visual Sci. **54**(12), 7293 (2013).
2. K. M. Meek and C. Knupp, "Corneal structure and transparency," Prog. Retinal Eye Res. **49**, 1–16 (2015).
3. G. Aurell and H. Holmgren, "On the metachromatic staining of the corneal tissue and some observations on its transparency," Acta Ophthalmol. **31**(1), 1–27 (2009).
4. D. M. Maurice, "The structure and transparency of the cornea," Journal of Physiology-London **136**(2), 263–286 (1957).
5. R. W. Hart and R. A. Farrell, "Light scattering in the cornea," J. Opt. Soc. Am. **59**(6), 766–774 (1969).
6. J. Goldman and G. Benedek, "The relationship between morphology and transparency in the nonswelling corneal stroma of the shark," Investigative Ophthalmology **6**, 574–600 (1967).
7. G. B. Benedek, "Theory of transparency of the eye," Appl. Opt. **10**(3), 459–473 (1971).
8. P. G. Watson and R. D. Young, "Scleral structure, organisation and disease: a review," Exp. Eye Res. **78**(3), 609–623 (2004).

Biomedical Optics EXPRESS

9. M. Han, G. Giese, and J. F. Bille, "Second harmonic generation imaging of collagen fibrils in cornea and sclera," Opt. Express **13**(15), 5791–5797 (2005).
10. S. Yamamoto, H. Hashizume, J. Hitomi, M. Shigeno, S. Sawaguchi, H. Abe, and T. Ushiki, "The subfibrillar arrangement of corneal and scleral collagen fibrils as revealed by scanning electron and atomic force microscopy," Arch. Histol. Cytol. **63**(2), 127–135 (2000).
11. A. Daxer, K. Misof, B. Grabner, A. Ettl, and P. Fratzl, "Collagen fibrils in the human corneal stroma: structure and aging," Investigative Ophthalmology and Visual Science **39**, 644–648 (1998).
12. Q. H. Liu, "Large-scale simulations of electromagnetic and acoustic measurements using the pseudospectral time-domain (PSTD) algorithm," IEEE Trans. Geosci. Remote Sensing **37**(2), 917–926 (1999).
13. S. H. Tseng, W. Ting, and S. Wang, "2-D PSTD Simulation of the time-reversed ultrasound-encoded deep-tissue imaging technique," Biomed. Opt. Express **5**(3), 882–894 (2014).
14. S. D. Gedney, "An anisotropic perfectly matched layer-absorbing medium for the truncation of FDTD lattices," IEEE Trans. Antennas Propag. **44**(12), 1630–1639 (1996).
15. Y. Huang, C. Tsai, and S. H. Tseng, "Simulating CW light propagation through macroscopic scattering media via optical phase conjugation," Journal of Applied Computational Electromagnetics Society **31**, 829–835 (2016).
16. D. L. Fried, "Optical resolution through a randomly inhomogeneous medium for very long and very short exposures," J. Opt. Soc. Am. **56**(10), 1372–1379 (1966).
17. R. K. Tyson, *Introduction to Adaptive Optics* (SPIE, 2000).
18. P. Léna, D. Rouan, F. Lebrun, F. Mignard, and D. Pelat, *Observational Astrophysics* (Springer Science & Business Media, 2012).
19. E. Hecht, *Optics* (Addison-Wesley, 2002).
20. W. Irvine and J. B. Pollack, "Infrared optical properties of water and ice spheres," Icarus **8**(1-3), 324–360 (1968).
21. G. Hale and M. Querry, "Optical constants of water in the 200 nm to 200 um wavelength region," Appl. Opt. **12**(3), 555–563 (1973).
22. A. Bashkatov, E. Genina, V. Kochubey, and V. Tuchin, "Optical properties of human sclera in spectral range 370–2500 nm," Opt. Spectrosc. **109**(2), 197–204 (2010).
23. Z. S. Sacks, R. M. Kurtz, T. Juhasz, and G. A. Mourau, "High precision subsurface photodisruption in human sclera," J. Biomed. Opt. **7**(3), 442–450 (2002).
24. E. A. Boettner and J. R. Wolter, "Transmission of the ocular media," Invest. Ophthalmol. Visual Sci. **1**, 776–783 (1962).
25. A. Abass, S. Hayes, N. White, T. Sorensen, and K. M. Meek, "Transverse depth-dependent changes in corneal collagen lamellar orientation and distribution," J. R. Soc. Interface. **12**(104), 20140717 (2015).